Resilient Unit Commitment for Transmission Lines Hardening Under Endogenous Uncertainties

Xiang Yang, Xinghua Liu, *Senior Member, IEEE*, Tianyang Zhao, *Senior Member, IEEE*, Gaoxi Xiao, *Senior Member, IEEE*, Bangji Fan, Shengwei Liu, *Graduate Student Member, IEEE*, and Peng Wang, *Fellow, IEEE*

***Abstract*—This paper proposes a joint strategy of pre-disaster hardening for transmission lines and real-time dispatching for units to address the failures with endogenous uncertainties caused by hurricanes on transmission lines. Specifically, we delve into the resilient unit commitment (UC) problem, which is formulated as a two-stage robust optimization (TRO) problem with endogenous uncertainty. In the first stage, the generator states, outputs, reserves, and line reinforcement are pre-scheduled to minimize defense costs. The second stage adopts a recourse approach to quantify the worst-case failure scenario of the lines, reflected as the costs of load shedding and generator curtailment. The operating status of transmission lines is depicted by an endogenous uncertainty set which is affected by the line hardening decision and unit reserve decision in the first stage. The TRO model with endogenous uncertainty is solved using a modified column-and-constraint generation (C&CG) algorithm. The proposed model is tested on two reliability test systems (RTS), including a modified IEEE RTS-79 and a two-area IEEE RTS-96 exposed to a hurricane. The results verify the effectiveness of the proposed method, compared with the popular two-stage robust optimization method with endogenous uncertainty.**

***Index Terms*—Unit commitment, transmission lines hardening, two-stage robust optimization, endogenous uncertainty.**

NOMENCLATURE

Indexes and Sets

$g \in \mathcal{G}$	Generator set.
$t \in \mathcal{T}$	Scheduling time set.
$ij \in \mathcal{L}$	Transmission line set.
$i, j \in \mathcal{B}$	Bus set.
$d \in \mathcal{D}$	Demand set.
$h \in W_{ij}$	Tower set of line ij.
$l \in K_{ij}$	Conductor segment set of line ij.

Parameters

$v_{h,s,t}$	Equivalent wind speed at tower h for the period t in the hurricane path s [m/s].
μ_h, σ_h	Mechanical losses expectation and variance values of the tower h.
$L_{ij,k}$	Line segment length [km].
$v_{ij,k,t}$, $V_{ij,k}$	Wind speed and design wind speed rates at the location of segment k [m/s].
$f_{ij,k,t}$, $F_{ij,k}$	Rainfall rate and design rainfall rate at the location of segment k [mm/h].
$a_{ij,k}$, $b_{ij,k}$, $c_{ij,k}$	Coefficient of the segment k of the line ij by wind speed, rainfall and other factors.
$c_{\text{start},g}$, $c_{\text{shut},g}$	Start-up and shut-down cost of generator g [$].
a_g, b_g	Fuel cost of generator g [$].
$c_{\text{R},g}$, $c^{+}_{r,g}$, $c^{-}_{r,g}$	Reserve cost of generator g [$/MWh].
c_{ij}	Hardening cost of line ij [$].
T^{R}_{ij}	Repair time of line ij [h].
$VOLL$	Load shedding cost of line ij [$/MWh].
$VOGC$	Curtailment cost of generator g [$/MWh].
T^{UP}_{g}, T^{DN}_{g}	Minimum up and down time of generator g [h].
T^{RU}_{g}, T^{RD}_{g}	Remaining up and down duration of generator g [h].
δ^{+}_{r}, δ^{-}_{r}, δ_R	Regulation up/down and spinning reserve requirement.
R^{60+}_{g}, R^{60-}_{g}	Maximum 60-min ramp up and ramp down rates of generator g [MW/h].
SU_g, SD_g	Start-up and shut-down ramp limitation of generator g [MW].
p^{t}_{g}	Active power output of generator g [MW].
P^{t}_{d}	Power demand [MW].
$B_{i,j}$	Susceptance of line ij [S].
$P^{\max}_{ij}$, $P^{\min}_{ij}$	Maximal and minimal power transfered on line ij [MW].
Δp^{t}_{d}	Variation of load d [MW].
π^{t}_{ij}	Failure probability of line ij in the t-th time slot.

Manuscript received 26 June 2023; revised 28 December 2023 and 6 April 2024; accepted 26 May 2024. Date of publication 29 May 2024; date of current version 27 December 2024. This work was supported in part by the Shaanxi Outstanding Youth Science Fund Project under Grant 2024JC-JCQN68, in part by the Future Resilient Systems Program (FRS-II) at the Singapore-ETH Centre (SEC), funded by National Research Foundation (NRF), Singapore, and in part by the High Level Talents Plan of Shaanxi Province for Young Professionals. Paper no. TPWRS-00982-2023. *(Corresponding authors: Xinghua Liu; Tianyang Zhao.)*

Xiang Yang, Xinghua Liu, and Bangji Fan are with the School of Electrical Engineering, Xi'an University of Technology, Xi'an 710048, China (e-mail: yangx@stu.xaut.edu.cn; liuxh@xaut.edu.cn; fanbj@stu.xaut.edu.cn).

Tianyang Zhao is with the School of Electrical Engineering, Xi'an Jiaotong University, Xi'an 710049, China (e-mail: zhaoty@xjtu.edu.cn).

Gaoxi Xiao and Peng Wang are with the School of Electrical and Electronic Engineering, Nanyang Technological University, Singapore 639798 (e-mail: egxxiao@ntu.edu.sg; epwang@ntu.edu.sg).

Shengwei Liu is with Energy Electricity Research Center, Jinan University, Zhuhai 519070, China (e-mail: 15622767651@163.com).

Color versions of one or more figures in this article are available at https://doi.org/10.1109/TPWRS.2024.3406712.

Digital Object Identifier 10.1109/TPWRS.2024.3406712

Π	Threshold of line ij failure probability.
K	Maximal number of failed lines in each time slot.
Δt	Time slot [h].
M	Big-M [1×10^{10}].

Uncertain Variables

$\gamma_{ij}^{t,0}$, γ_{ij}^{t}	Binary variable of line ij failure state before and after hardening measures in the t-th time slot: 1 if line ij is failed; 0 otherwise.
κ_{ij}^{t}	Binary variable of line ij repair state in the t-th time slot: 1 if line ij is repaired; 0 otherwise.
I_{ij}^{t}	Binary variable of line ij operating state in the t-th time slot: 1 if line ij is on-line; 0 otherwise.

First Stage Decision Variables

α_g^t, β_g^t, u_g^t	Binary variable of generator g start-up command, shut-down command, and operating state in the t-th time slot.
P_g^t, R_g^t	Power output and spinning reserve of generator g [MW].
$r_g^{+,t}$, $r_g^{-,t}$	Spinning up and spinning down reserve of generator g [MW].
θ_i^t	Impedance angle at bus i [°].
Q_{OR}^t	Operating reserve [MW].
P_{ij}^t	Power transmitted on line ij [MW].
x_{ij}	Binary variable of line ij hardening action: 1 if line ij is reinforced; 0 otherwise.

Second Stage Decision Variables

p_d^t	Shedding of load d [MW].
$p_{\text{cur},g}^t$	Curtailment of generator g [MW].
γ_i^t	Angle at bus i [°].
p_{ij}^t	Power transmitted on line ij [MW].

I. Introduction

A. Background and Motivation

HURRICANES, also called typhoons, are extreme natural disasters that threaten the secure and reliable operation of power systems. To effectively respond to such high-impact-low-probability (HILP) extreme events, it is vital to enhance power system resilience. The measures to enhance power system resilience in response to extreme events can be classified into three categories by their respective implementation time: "resilience-based planning", "resilience-based response", and "resilience-based restoration" [1]. To improve the power system's ability to cope with an uncertain environment before hurricane attacks, a UC problem was formulated for resilience-enhancing scheduling [2]. Robust optimization (RO) is a method for making decisions under uncertainty, usually by constructing uncertainty factors as uncertainty sets. Earlier work on RO was limited to the static cases [3], which only considered decisions that needed to be made beforehand the decision making therefore has limitations. By quantifying the impact of hurricanes on transmission lines as line failure and operational status within the uncertainty set. Before the hurricane arrives, defensive hardening actions coupled with the newly constructed uncertainty set for transmission lines in this paper enable the uncertainty set to change as the decision is varied in a dynamic working state. Therefore, the defensive hardening decisions made from uncertainty sets constructed in this paper, i.e., the endogenous uncertainty set, will be an effective strategy to enhance the power system's resilience.

B. Related Works

Many scholars have studied the problem formulations and solutions in planning and operation for enhancing power system's resilience. Before extreme disaster events, the key to a resilient power system is prevention and preparation to promptly update vulnerable infrastructure. Reference [4] proposed adopting defensive islanding as a preventive measure to enhance the power system's resilience by maintaining critical load supply and avoiding cascading failures. During disaster events, the target for resilient power systems is to quickly adjust and respond to unforeseen situations. Ding et al. [5] proposed a three-stage resilient UC model, which can coordinate control strategies at the prevention, emergency, and recovery stages. During hurricanes, emergency control is conducted by taking local load shedding measures to achieve power balance quickly. Post-disaster resilience operations primarily involve the restoration and reconstruction of the power system to restore the power supply. Reference [6] proposed a method for coordinated restoration of electric bus dispatch and post-disaster distribution systems to accelerate the recovery process.

Proactive scheduling of the power system is also an essential aspect of boosting the power system's resilience. With extreme events attacking the power system, the operational uncertainty of the power system is further increased, aggravating the difficulty of decision-making in the proactive scheduling of the power system. According to the optimization method for handling uncertainty, two-stage robust, stochastic, and distributionally robust UC problems [7], [8], [9] were presented for achieving the resilient dispatch of power systems to improve the reliability and operational efficiency. Besides, preventive dispatch of emergency resources is an essential measure to reduce system losses during disasters. Distributed energy sources were adopted to restore critical loads in [10]. Reference [11] coordinated the dispatch of repair crews, mobile power sources, renewable energys, and energy storage systems to achieve system service restoration aiming at maximizing the amount of restored load. The previous uncertainties are constructed as decision-independent uncertainty (DIU), i.e., exogenous uncertainty [12].

The impact of hurricanes on transmission lines and demand-side response have strong uncertainties that raise significant challenges in resilient power system scheduling. The level of such uncertainty may depend on the strategy chosen by the decision maker, termed as decision-dependent uncertainty (DDU), i.e., endogenous uncertainty [13]. A two-stage robust economic dispatch model based on DDUs with demand response was proposed in [14], where the uncertainty set of demand response varies with the decision. In the stochastic optimization (SO) problem, the contingencies of transmission lines have been

modeled as continuous and discrete probability density functions (PDFs). In [15], the failure PDFs of transmission lines with tower damages and windage yaw flashovers during typhoon disasters were modeled respectively, which were applied to a two-stage SO under DDU. RO methods also have certain advantages in handling uncertainty issues. The impact of hurricanes on transmission lines requires to be constructed as uncertainty sets in RO [16]. Still, it is not dependent on the decision and is exogenous uncertainty, which needs to be further constructed as a DDU set.

Previous methods for solving the TRO model with exogenous uncertainty include sample average approximation algorithm [17], C&CG algorithm [18] and Benders decomposition algorithm. Reference [19] utilized the Benders decomposition method to tackle a TRO problem with DIU. In [20] and [21], enhanced Benders decomposition algorithms were applied to solve the two-stage optimization problem with DDU by incorporating dual cuts and primal cuts into the master problem, respectively. Furthermore, a theoretical approach of the modified Benders method for discrete uncertain events was proposed in [22], [23], simultaneously adding primal and dual cuts to the master problem. If the uncertain variables belong to the 0-1 variables, the modified Benders decomposition algorithm cannot be directly adopted because the strong dual principle will not be applied. In addition, the variants of classical C&CG algorithm [24] could also solve the TRO with DDU. The first variant of the classical C&CG algorithm solves uncertain variables by enumeration. Although it is theoretically reasonable, its performance in searching for the worst-case scenario and the convergence speed is unsatisfactory even for small-scale examples. Accordingly, the algorithm can be further improved and extended to improve its performance.

C. Contributions and Organization

To cope with the problem that the hardening of one line will affect the state of other lines in the power system, this paper proposes a TRO model with endogenous uncertainty for the states and reinforcements of transmission lines. This endogenous uncertainty set is integrated into a TRO problem that considers generator start-up, shut-down, fuel, reserve, and hardening costs in the first stage. The second stage considers load shedding and generator curtailment penalty costs, which are formulated as recourse problems to balance the economic efficiency and robustness of the system. The key contributions of this paper can be summarized as follows

1) An advanced endogenous polyhedral uncertainty set is established to precisely quantify the influence of extreme events on transmission lines, particularly in the context of hardening lines and unit reserve under hurricanes. Distinguished from previous studies [25], [26], the proposed uncertainty set outperforms its rivals in reflecting real-world scenarios.
2) To address the challenges of power system resilience under hurricanes, we put forth a novel TRO problem to minimize the proactive scheduling costs, where the unit commitments planning and hardening measures for lines can be optimized within the warning window period leading up to the arrival of a hurricane. Based on the cooperative gaming experiment with line hardening and unit commitment schemes, we achieve results that the strategies proposed in this paper could compensate for each other and improve resilience jointly.
3) A modified C&CG algorithm is proposed to solve the TRO problem by adeptly employing inverse initialization and endogenous cuts. Simulation results show that this innovative approach possesses a heightened sensing capability of line faults and high computational efficiency in disaster prevention and mitigation compared with the Benders + C&CG [24] and C&CG-AOP algorithms [27].

The rest of this paper is organized as follows. TRO on the resilient unit commitment is formulated in Section II. The optimization problem is solved by the modified C&CG algorithm in Section III. In Section IV, the case study is performed and simulation results are analyzed. Conclusions are summarized in Section V.

II. Resilient Unit Commitment Considering Transmission Lines Hardening

The transmission lines hardening under endogenous uncertainty is formulated as a TRO problem. The first stage is to make the unit's operational decisions and the hardening decisions for the transmission lines. The second stage considers load shedding and generator curtailment, formulating a recourse problem based on the worst-case situation of the endogenous uncertainty set. In the optimization model, only the impact of hurricane disasters on transmission lines is considered.

A. Objective Function

The objective function is to minimize the proactive scheduling costs of generator start-up, shut-down, fuel, reserve and transmission line hardening, as well as the worst-case load shedding penalties cost considering the failure and operation status of the transmission line, as follows:

$$\min_{\mathbf{x}\in\mathbf{X}}\left\{f(\mathbf{x})+\max_{\mathbf{u}\in\mathcal{U}(\mathbf{x})}\mathcal{Q}(\mathbf{x})\right\} \tag{1}$$

$$\begin{aligned} f(\mathbf{x}) &= \mathbf{c}^{\mathrm{T}}\mathbf{x} \\ &= \sum_{t\in\mathcal{T}}\sum_{g\in\mathcal{G}}\{\underbrace{c_{\text{start},g}\alpha_g^t+c_{\text{shut},g}\beta_g^t}_{\text{start-up and shut-down cost}}+\underbrace{b_g u_g^t+\left[a_g P_g^t\right.}_{\text{fuel cost}} \\ &\quad+\underbrace{c_{\mathrm{R},g}R_g^t+c_{r,g}^{+}r_g^{+,t}+c_{r,g}^{-}r_g^{-,t}]}_{\text{reserve cost}}\Delta t\}+\sum_{ij\in\mathcal{L}}\underbrace{c_{ij}x_{ij}}_{\text{harden cost}} \end{aligned} \tag{2}$$

$$\begin{aligned} \mathcal{Q}(\mathbf{x}) &= \min_{\mathbf{y}\in\mathcal{Y}(\mathbf{x},\mathbf{u})}\mathbf{d}^{\mathrm{T}}\mathbf{y} \\ &= \sum_{t\in\mathcal{T}}\left(VOLL\sum_{d\in\mathcal{D}}p_d^t+VOGC\sum_{g\in\mathcal{G}}p_{\text{cur},g}^t\right)\Delta t \end{aligned}$$

$$\text{s.t.}\quad \mathbf{Ax}\le\mathbf{b},\mathbf{Ey}\ge\mathbf{h}-\mathbf{Gx}-\mathbf{Mu},\mathbf{Cu}\le\mathbf{g}+\mathbf{Nx} \tag{3}$$

where $\mathbf{x}:=\{\alpha_g^t,\beta_g^t,u_g^t,P_g^t,R_g^t,r_g^{+,t},r_g^{-,t},\theta_i^t,P_{ij}^t,Q_{OR}^t,x_{ij}\}$ is the first-stage decision variable vector. $f(\mathbf{x})$ is the system

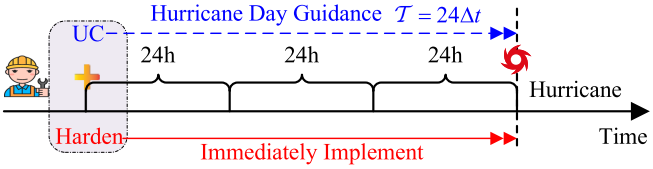

Fig. 1. Timeframe diagram for line hardening and UC.

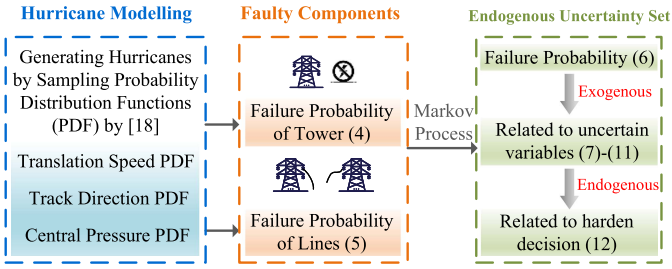

Fig. 2. Procedure for constraints derivation of endogenous uncertainty set.

operation cost. $\mathbf{y} := \{p_d^t, p_{\text{cur},g}^t, \gamma_i^t, p_{ij}^t\}$ is the second-stage decision variable vector. $\mathbf{u}$ is the uncertain variable vector for TRO. $\mathbf{X}$ is a vector set consisting of the constraints satisfied by the decision in the first stage. $\mathcal{Y}(\mathbf{x}, \mathbf{u})$ is the vector set consisting of the constraints satisfied by the elements in $\mathbf{y}$ for the real-time operation of power systems after the realization of uncertainties. $\mathcal{U}(\mathbf{x})$ is the endogenous uncertainty set. $\mathbf{c}$ and $\mathbf{d}$ are coefficient vectors for the first and second stage objective function, respectively.

Remark 1: The timeframe diagram for the line hardening and UC plans is shown in Fig. 1 . With the current capability of forecasting hurricane landfall by the meteorological department, a 72-hour advance warning can be achieved. Then, the temporary hardening measures can be implemented within this time window. Note that x_{ij} is independent of Δt, reflecting implementation or non-implementation of the actions such as vegetation management and pole upgrades [28], [29]. On the day of the hurricane, unit on/off planning serves as a reference for dispatchers, which makes a proactive defence. The temporary planning decision for line hardening and operational decisions of unit are formulated within the same phase [30], [31].

B. Endogenous Uncertainty set

In this subsection, we quantify the impact of hurricanes on transmission lines by using the failure probability. These probabilities, along with other uncertain variables, are included as constraints in an endogenous uncertainty set. Fig. 2 illustrates the constraint derivation process for the endogenous uncertainty set.

1) Impact of Hurricanes on Transmission Line Failures: A hurricane can be defined as a cyclone that moves in a given time and space. Hurricanes could cause damage to lines, transformers, substations and other equipment within the power system. When factors such as associated flooding are not considered, the damage is mainly caused by transmission line failures [32]. For modeling hurricanes, this paper simulates the path of a hurricane by sampling the hurricane's translation speed, track direction, and centre pressure deficit probability distribution function [16]. In terms of geographic data, the location of exposed components and local topographic features are considered. The hurricane event data consists of the time-varying hurricane position, movement direction and speed, maximum sustained wind speed, and minimum central pressure [33]. The simulation assumes that the translational speed, track direction, and central pressure follow lognormal, normal, and lognormal distributions, which are based on the corresponding parameters, respectively.

Elevated transmission lines are composed of elements such as towers and lines. For a tower h, the probability of its failure $\pi_{h,s}^t$ under a hurricane path s can be expressed as follows [34]

$$\pi_{h,s}^t = \int_{-\infty}^{v_{h,s,t}} \frac{1}{\sigma_h \sqrt{2\pi}} \exp\left(\frac{-(x-\mu_h)^2}{2\sigma_h^2}\right) \mathrm{d}x \tag{4}$$

The probability of failure $\pi_{ij,l,s}^t$ of the l conductor segment about transmission line ij can be expressed as follows

$$\pi_{ij,l,s}^t = L_{ij,k} \exp\left(\frac{a_{ij,k} v_{ij,k,t}}{V_{ij,k}} + \frac{b_{ij,k} f_{ij,k,t}}{F_{ij,k}} + c_{ij,k}\right) \tag{5}$$

By modeling the probability of failure $\pi_{ij,s}^t$ for the line ij as a discrete Markov process [33], its probability can be derived as follows

$$\pi_{ij,s}^t = 1 - \prod_{h \in W_{ij}} \left(1 - \pi_{h,s}^t\right) \prod_{l \in K_{ij}} \left(1 - \pi_{ij,l,s}^t\right) \tag{6}$$

2) Model of Endogenous Uncertainty set: Considering the impact of hurricanes on transmission, the operation, failure and repair status of transmission lines are treated as uncertainty factors. Since there is a certain relation between the decision x_{ij} of whether to harden the transmission line in the first stage and the line fault state γ_{ij}^t, they constitute an endogenous uncertainty constraint. The uncertainty set, i.e., $\mathcal{U}(\mathbf{x}) := \{\mathbf{u} \in \{0,1\}^{m_u} \mid \mathbf{C}\mathbf{u} \leq \mathbf{g} + \mathbf{N}\mathbf{x}\}$, is depicted as a polyhedral model.

Considering the failure probability of a line in hurricane in (6), the following constraints are employed to detect which lines shall be affected by the hurricane during which time period using threshold Π [16].

$$\gamma_{ij}^{t,0} \left(\pi_{ij,s}^t - \Pi\right) \geq 0, \forall t, ij \tag{7}$$

This relation of failure, repair, and the status transition of line ij can be depicted by the following equation.

$$\kappa_{ij}^t - \gamma_{ij}^t = I_{ij}^t - I_{ij}^{t-1}, \forall t, ij \tag{8}$$

Each line ij can be damaged at most once in a dispatch cycle [35], which is described as follows

$$\sum_{t \in \mathcal{T}} \gamma_{ij}^t \leq 1, \forall t, ij \tag{9}$$

During each time slot $t \in \mathcal{T}$, at most K transmission lines are allowed to be destroyed simultaneously [16], as follows

$$\sum_{ij \in \mathcal{L}} I_{ij}^t \geq |\mathcal{E}| - K, \forall t, ij \tag{10}$$

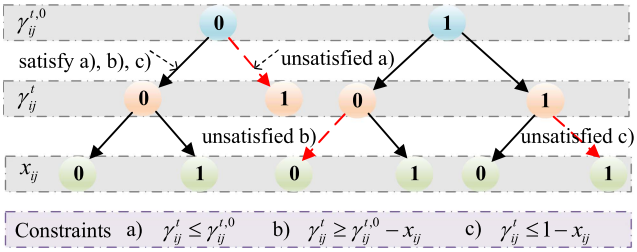

Fig. 3. A diagram of the values of $\gamma_{ij}^{t,0}$, γ_{ij}^{t}, and x_{ij}.

For (8), the definite restoration time limitation needs to be satisfied if the post-disaster repair action κ_{ij}^{t} for the failed line is considered. Hence, the constraint is constructed as follows

$$\kappa_{ij}^{t+\mathrm{T}_{ij}^{R}} = \chi_{ij}^{t}, \forall t \in \left\{1, 2, \ldots, T - \mathrm{T}_{ij}^{R}\right\}, ij \tag{11}$$

The hardening decision x_{ij} in the first stage is coupled with uncertain variables, specifically the pre-reinforcement and post-reinforcement fault states, which is formulated as follows

$$\gamma_{ij}^{t,0} - x_{ij} \le \gamma_{ij}^{t} \le \min\left\{\gamma_{ij}^{t,0}, 1 - x_{ij}\right\}, \forall t, ij \tag{12}$$

Constraint (12) is derived from the constraints a), b), and c) illustrated in Fig. 3, involving potential values for the states $(\gamma_{ij}^{t,0}, \gamma_{ij}^{t}, x_{ij}) \in \{0, 1\}$. In Fig. 3, three scenarios marked with red arrows are undesired, and their limitations are respectively marked with black dashed arrows. The four cases of (12) are shown as follows

- Case 1 $(\gamma_{ij}^{t,0}, \gamma_{ij}^{t}, x_{ij}) = (0, 0, 0)$ represents that the line is not damaged by the hurricane and therefore not hardened.
- Case 2 $(\gamma_{ij}^{t,0}, \gamma_{ij}^{t}, x_{ij}) = (0, 0, 1)$ describes that the line is not damaged by the hurricane but hardened, which should be optimized to align with Case 1.
- Case 3 $(\gamma_{ij}^{t,0}, \gamma_{ij}^{t}, x_{ij}) = (1, 0, 1)$ represents that the line is damaged by the hurricane, necessitating hardening to ensure post-reinforcement fault-free operation.
- Case 4 $(\gamma_{ij}^{t,0}, \gamma_{ij}^{t}, x_{ij}) = (1, 1, 0)$ describes that the line is damaged by the hurricane both before and after reinforcement, resulting in no effective hardening.

Notably, $(\gamma_{ij}^{t,0}, \gamma_{ij}^{t}, x_{ij}) = (1, 1, 1)$ is not realistic since the line still fail after hardening and there is cost of hardening. Thus, $\gamma_{ij}^{t,0} \le 1 - x_{ij}$ is introduced to avoid such case.

Remark 2: A 0-1 variable ϖ^{t} is introduced in the first stage to indicate whether the unit is on reserve or not. The endogenous uncertainty of the line failure after hardening γ_{ij}^{t} and UC reserve thus can be considered, which is formulated as follows

$$\varpi^{t} \ge \sum_{ij \in \mathcal{L}} \gamma_{ij}^{t}, \forall t, ij \tag{13}$$

Remark 3: Compared to the ordinary uncertainty set of static transmission line states, the proposed endogenous uncertainty set characterizes the line states as time-varying variables, providing a more accurate depiction of the temporal evolution of the transmission line. In contrast to the exogenous uncertainty set [16], the proposed endogenous set posits that the fault status of the line is influenced by hardening measures, emphasizing the time-varying impact of reinforcement on transmission line faults under hurricanes. Distinguished from unrelated uncertain variables in an uncertainty set [26], the proposed endogenous set defines the states of line damage, repair, and operation as correlated uncertain variables, offering a more comprehensive description of the evolving process of line states. Meanwhile, the proposed model acknowledges the possibility of hurricane-induced damage to reinforced transmission lines. Therefore, the proposed endogenous uncertainty set is more applicable for reflecting real-world scenarios.

C. Constraint Set of the First Stage

The constraint set of the first stage, i.e., $\mathbf{X} := \{\mathbf{x} \in \mathbb{R}^{m_x} \times \{0, 1\}^{n_x} \mid \mathbf{A}\mathbf{x} \le \mathbf{b}\}$, which includes the technical constraints of generators, transmission lines, power balance and reserve requirements [16], are formulated as follows:

1) Logic Constraint: The logic constraints describe the relationship between the operating state and the start-up/shut-down command of the generator.

$$\alpha_g^t - \beta_g^t = u_g^t - u_g^{t-1}, \alpha_g^t + \beta_g^t \le 1, \forall t, g \tag{14}$$

$$u_g^t = u_g^0, \forall t \in \left\{\Delta t, \ldots, \mathrm{T}_g^{RU} + \mathrm{T}_g^{RD}\right\}, g \tag{15}$$

2) Start-up/Shut-Down Time Constraint: Each generator requires the minimum up/down time to start-up or shut-down due to the physical limit, the constraints are shown as follows.

$$\sum_{q=t-\mathrm{T}_g^{UP}+1}^{t} \alpha_g^q \le u_g^t, \forall t \in \left\{\mathrm{T}_g^{UP}, \ldots, T\right\}, g \tag{16}$$

$$\sum_{q=t-\mathrm{T}_g^{DN}+1}^{t} \beta_g^q \le 1 - u_g^t, \forall t \in \left\{\mathrm{T}_g^{DN}, \ldots, T\right\}, g \tag{17}$$

3) Ramping Rate Constraint: The ramping capability of the generator g is constrained by the allowable upward SU_g and downward SD_g rates, the constraints are formulated as

$$P_g^t - P_g^{t-1} \le \mathrm{R}_g^{60+} u_g^{t-1} \Delta t + \alpha_g^t \mathrm{SU}_g, \forall t, g \tag{18}$$

$$P_g^{t-1} - P_g^t \le \mathrm{R}_g^{60-} u_g^t \Delta t + \beta_g^t \mathrm{SD}_g, \forall t, g \tag{19}$$

4) Reserve Constraint: The capacity reserve constraint of the generator is expressed as follows (see [36] for more details).

$$u_g^t P_g^{\min} \le P_g^t - r_g^{-,t}, 0 \le R_g^t \le \mathrm{R}_g^{10+} u_g^t, \forall t, g \tag{20}$$

$$P_g^t + R_g^t + r_g^{+,t} \le P_g^{\max} u_g^t, \forall t, g \tag{21}$$

$$0 \le r_g^{-,t} \le \mathrm{R}_g^{5-} u_g^t, 0 \le r_g^{+,t} \le \mathrm{R}_g^{5+} u_g^t, \forall t, g \tag{22}$$

$$Q_{\mathrm{OR}}^t \ge P_g^t + R_g^t, \sum_{g \in \mathcal{G}} R_g^t \ge \delta_{\mathrm{R}} Q_{\mathrm{OR}}^t, \forall t, g \tag{23}$$

$$\sum_{g \in \mathcal{G}} r_g^{+,t} \ge \delta_r^{+} \sum_{d \in \mathcal{D}} P_{d,j}^t, \sum_{g \in \mathcal{G}} r_g^{-,t} \ge \delta_r^{-} \sum_{d \in \mathcal{D}} P_{d,j}^t, \forall t, g \tag{24}$$

5) Power Flow Constraint: The constraints of power balance and power flow for each transmission line are formulated as

$$\sum_{g \in \mathcal{G}_j} P_g^t + \sum_{ij} P_{ij}^t - \sum_{ji} P_{ji}^t = \sum_{d \in \mathcal{D}_j} P_d^t, \forall t, j \tag{25}$$

$$P_{ij}^t - B_{ij}\left(\theta_i^t - \theta_j^t\right) = 0, \forall t, ij \tag{26}$$

$$P_{ij}^{\min} \le P_{ij}^t \le P_{ij}^{\max}, \forall t, ij \tag{27}$$

D. Constraint Set of the Second Stage

The second stage constraint set, i.e., $\mathcal{Y}(\mathbf{x},\mathbf{u}) := \{\mathbf{y} \in \mathbb{R}^{m_y} \mid \mathbf{E}\mathbf{y} \ge \mathbf{h} - \mathbf{G}\mathbf{x} - \mathbf{M}\mathbf{u}\}$, includes constraints on the real-time scheduling of generators, power flow, load shedding, generation curtailment, as follows.

1) Generator Dispatch and Power Balance Constraints: The scheduling of the generator, governed by (28), is subject to its physical limitations. During a hurricane, adjustments to the unit g schedule enable the shedding of load demand, ensuring bus power balance as (29).

$$P_g^t - R_g^t \le p_g^t \le P_g^t + R_g^t, \forall t, g \tag{28}$$

$$\sum_{g\in\mathcal{G}_j}\left(p_g^t - p_{\text{cur},g}^t\right) + \sum_{ij} p_{ij}^t - \sum_{ji} p_{ji}^t = \sum_{d\in\mathcal{D}_j}\left(P_d^t + \Delta p_d^t - p_d^t\right), \forall t, ij, j \tag{29}$$

2) Power Flow Constraint: The second stage is coupled with the endogenous uncertainty set. Hence, the line operating state variable I_{ij}^t of the uncertainty set is inserted in the power flow constraints of the second stage, which are expressed as follows

$$p_{ij}^t - B_{ij}\left(\gamma_i^t - \gamma_j^t\right) \ge \left(I_{ij}^t - 1\right)P_{ij}^{\max}, \forall t, ij \tag{30}$$

$$p_{ij}^t - B_{ij}\left(\gamma_i^t - \gamma_j^t\right) \le \left(1 - I_{ij}^t\right)P_{ij}^{\max}, \forall t, ij \tag{31}$$

$$-I_{ij}P_{ij}^{\max} \le p_{ij}^t \le I_{ij}P_{ij}^{\max}, \forall t, ij \tag{32}$$

3) Load Shedding/Generator Curtailment Constraint: As the impact of extreme events, both load demand and generator output will vary [35], which is depicted as follows

$$P_d^t + \Delta p_d^t \ge p_d^t \ge 0, \forall t, d \tag{33}$$

$$p_g^t \ge p_{\text{cur},g}^t \ge 0, \forall t, g \tag{34}$$

Remark 4: We assume that the problem (1) has relatively complete recourse, i.e., for any $\mathbf{x} \in \mathbf{X}$ and $\mathbf{u} \in \mathcal{U}(\mathbf{x})$, the set $\mathcal{Y}(\mathbf{x},\mathbf{u})$ is non-empty. This means that all generators can be curtailed and each load can be shedded.

III. Solution Methods

The formulated problem (1) is a typical TRO with an endogenous uncertainty set. The first stage is a mixed integer linear programming (MILP) problem. The second stage is a max-min problem, of which the inner layer is a linear programming problem and is always feasible. However, since the uncertainty set is endogenous and changes during each iteration of the master problem (MP) and subproblem (SP), we make the following two improvements to the classical C&CG algorithm to tackle the problem.

- A heuristic as an improvement to the initialization of the algorithm. Such an approach ensures that Algorithm 1 initially obtains a valid lower boundary, thereby expediting subsequent identification of the worst-case and facilitating more efficient decision-making processes.
- Apart from the existing primal cuts in the master problem [18], we introduce an additional cut, named endogenous cut, whose specific objectives is depicted in Section III-B.

These two innovative approaches play complementary roles. The specific algorithm process is described in Algorithm 1.

A. Initialization of Algorithm

In the initialization of the algorithm, we invert the coefficients of the decision variables coupled with the endogenous uncertainty set in the first stage. That is, the following mathematical model is solved.

$$\min_{\mathbf{x}\in\mathbf{X}}\left\{-\mathbf{c_1^T}\mathbf{x} + \max_{\mathbf{u}\in\mathcal{U}(\mathbf{x})}\min_{\mathbf{y}\in\mathcal{Y}(\mathbf{x},\mathbf{u})}\mathbf{d}^{\mathrm{T}}\mathbf{y}\right\}$$
$$\text{s.t.}\quad \mathbf{A}\mathbf{x} \le \mathbf{b}, \mathbf{E}\mathbf{y} \ge \mathbf{h} - \mathbf{G}\mathbf{x} - \mathbf{M}\mathbf{u}, \mathbf{C}\mathbf{u} \le \mathbf{g} + \mathbf{N}\mathbf{x} \tag{35}$$

By introducing a heuristic reverse initialization process, Algorithm 1, with the increase of iteration, results in non-increase and non-decrease series of $|\mathbf{x}_k^*| \le |\mathbf{x}_{k-1}^*|$ and $|\mathbf{u}_k^*| \ge |\mathbf{u}_{k-1}^*|$, as demonstrated in Lemmas 1 and 2. In contrast to the ordinary C&CG [18], where iterations lead to $|\mathbf{x}_k^*| \ge |\mathbf{x}_{k-1}^*|$ and $|\mathbf{u}_k^*| \le |\mathbf{u}_{k-1}^*|$, the reverse iteration strategy in Algorithm 1 enables more rapid identification of the worst-case for TRO and corresponding decision-making in the first stage.

Remark 5: During hurricanes, minimizing the operational risk is paramount for a power system. This paper endeavors to investigate the defense and mitigation strategies for power systems during hurricanes, which triggers the motivation of incorporating inverse initialization into the C&CG algorithm. The merit of the inverse initialization approach lies in solving the TRO with the starting point of minimizing the operational risk and maximizing the defense cost for the power system.

The following dual approach is used to solve the second stage problem, i.e., $\max_{\mathbf{u}\in\mathcal{U}(\mathbf{x})}\mathcal{Q}(\mathbf{x})$. Let π be a dual variable. Then, the dual process for $\mathcal{Q}(\mathbf{x})$ is a maximization problem, which can be merged with the maximization for $\mathbf{u}$.

$$S(u) = \max_{\mathbf{u},\pi}(\mathbf{h} - \mathbf{G}\mathbf{x} - \mathbf{M}\mathbf{u})^{\mathrm{T}}\pi \tag{36a}$$

$$\text{s.t.}\quad \mathbf{E}^{\mathrm{T}}\pi \le \mathbf{d}, \pi \ge \mathbf{0}, \mathbf{C}\mathbf{u} \le \mathbf{g} + \mathbf{N}\mathbf{x} \tag{36b}$$

Note that the problem produced in (36) is a bilinear optimization problem. Considering that $\mathbf{u}$ is a binary vector, non-convex quadratic term $\mathbf{u}^{\mathrm{T}}\mathbf{M}^{\mathrm{T}}\pi$ can be exactly reformulated using its McCormick envelop [37].

B. Cut Sets of Algorithm

1) Primal cut: The convergence speed of the modified C&CG algorithm, i.e., the variation degree of LB and UB per update, is strongly influenced by the cut set added to the master problem each cycle. As shown in rows 18 to 27 of Algorithm 1, the cut set is updated by the extreme value point or extreme value ray of the subproblem (36) to form the optimal cut and the feasible cut. The dual cutting plane converges slowly due to the

Algorithm 1: Modified C&CG Algorithm for Two-Stage Robust UC Under Endogenous Uncertainties.

Input: X, $\mathcal{Y}(\mathbf{x},\mathbf{u})$, $\mathcal{U}$, $\mathbf{c}$, $\mathbf{d}$, ε
Output: $\mathbf{x}$, $\mathbf{y}$, $\mathbf{u}$
1 Set $LB^0=-\inf$, $UB^0=\inf$ and k=1
2 **while** $k \le k_{max}$ **do**
3 $\star\star\star\star$ **Initialization Step** $\star\star\star\star$
4 **if** $k=1$ **then**
5 Solve the initialization problem (35)
6 **else**
7 Solve the master problem (MP)

$$\text{MP: } \min_{\mathbf{x},\eta,\mathbf{y}^k} \mathbf{c}^{\mathrm{T}}\mathbf{x}+\eta$$
$$\text{s.t. } \mathbf{x}\in\mathbf{X}, \eta \ge \mathbf{d}^{\mathrm{T}}\mathbf{y}^k, \eta\in\mathbb{R}$$
$$\mathbf{G}\mathbf{x}+\mathbf{E}\mathbf{y}^k \ge \mathbf{h}-\mathbf{M}\mathbf{u}^{k-1,*}$$

8 **end**
9 **if** *problem (MP) or problem (35) is infeasible* **then**
10 Terminate
11 **else**
12 Derive an optimal solution $\mathbf{x}^k$ and update $LB^k=\max\{LB^{k-1}, \text{objective value of MP}\}$
13 Derive $\mathbf{u}^{k,*}$, $\mathcal{Q}(\mathbf{x}^k)$ by solving (36) and update $UB^k=\min\{\mathbf{c}^{\mathrm{T}}\mathbf{x}^k+\mathcal{Q}(\mathbf{x}^k), UB^{k-1}\}$
14 **if** $(UB^k-LB^k)/\max(UB^k,LB^k)\le\varepsilon$ **then**
15 Return $\mathbf{x}^k$, $\mathbf{u}^{k,*}$ and terminate
16 **else**
17 $\star\star$ **Add Endogenous Cuts Step** $\star\star$
18 **if** *problem (36) has extreme point* **then**
19 Create variables $\mathbf{y}^{k+1}$ and add the following optimality cuts to MP
20 $\eta \ge \mathbf{d}^{\mathrm{T}}\mathbf{y}^{k+1}$
21 $\mathbf{G}\mathbf{x}+\mathbf{E}\mathbf{y}^{k+1}\ge\mathbf{h}-\mathbf{M}\mathbf{u}^{k,*}$
22 $\mathbf{C}\mathbf{u}^{k,*}\le\mathbf{g}+\mathbf{N}\mathbf{x}$
23 **else if** *problem (36) has extreme ray* **then**
24 Create variables $\mathbf{y}^{k+1}$ and add the following feasibility cuts to MP
25 $0 \ge \mathbf{d}^{\mathrm{T}}\mathbf{y}^{k+1}$
26 $\mathbf{G}\mathbf{x}+\mathbf{E}\mathbf{y}^{k+1}\ge\mathbf{h}-\mathbf{M}\mathbf{u}^{k,*}$
27 $\mathbf{C}\mathbf{u}^{k,*}\le\mathbf{g}+\mathbf{N}\mathbf{x}$
28 **end**
29 Update $k=k+1$
30 **end**
31 **end**
32 **end**

large number of cuts required to approximate the cost function $\mathcal{Q}(\mathbf{x})$. The optimal solution of problem (36), i.e., $\mathbf{u}^{k,*}$, is used to introduce a new primal cut for the master problem in each iteration [38].

$$\eta \ge \mathbf{d}^{\mathrm{T}}\mathbf{y}^{k+1}, \mathbf{G}\mathbf{x}+\mathbf{E}\mathbf{y}^{k+1}\ge\mathbf{h}-\mathbf{M}\mathbf{u}^{k,*} \tag{37}$$

2) Endogenous cut: With the introduction of the primal cut, we incorporate the endogenous uncertainty set as a cut plane into the master problem of the Algorithm 1.

$$\mathbf{C}\mathbf{u}^{k,*}\le\mathbf{g}+\mathbf{N}\mathbf{x} \tag{38}$$

Compared to the purposes of endogenous cuts in MP [23], [24], the endogenous cuts in Algorithm 1 have three objectives: (1) Since the cut plane in the MP is related to $\mathbf{u}$, while $\mathbf{u}$ is solved in the SP and depends on $\mathbf{x}$. Thus, the introduced endogenous cut ensures the feasibility of the MP; and (2) the TRO searches for the worst case that is the vertices of uncertain polyhedral set. As the uncertainty set is endogenous, the set of vertices of the polyhedron changes with $\mathbf{x}$, while $\mathbf{x}$ varies with the number of iterations. Thus, the introduced endogenous cut ensures the finite convergence of Algorithm 1; and (3) due to the heuristic inverse initialization operation in $k=1$, the solution $\mathbf{x}_1$ obtained for the MP is exactly opposite to the expected result. Therefore, the introduced endogenous cut ensures that $\mathbf{x}$ is updated when $k\ge 2$.

Remark 6: The worst failures of the power system include line tripping, generators off-grid, and abrupt load variation under hurricanes. The worst case under the hurricane mentioned in this paper is to maximize the number of damaged lines $\sum_{t\in\mathcal{T}}\sum_{ij\in\mathcal{L}}\gamma_{ij}^{t,0}$ before reinforcement. Suppose that Algorithm 1 terminates at the N-th iteration, the $\mathbf{u}^{N,*}$ solved by (36) is the overall worst case. The decision $\mathbf{x}^{N,*}$ solved by the MP at the N-th iteration is the overall optimal plan [39].

Lemma 1: If $\mathbf{c}$ is non-negative and $\mathbf{x}_k^*$ is an exact solution in the MP, then as the increase of iteration, $|\mathbf{x}_k^*|\le|\mathbf{x}_{k-1}^*|$, leading to a non-increase series of lower boundary.

Proof: Let $\mathbf{x}_k^*$ denote the line hardening decision in the first stage decision variable at iteration k. Since $\mathbf{c}$ is non-negative when $k=1$, in Line 5 of Algorithm 1, deriving $\mathbf{x}_1^*=[1,1,\ldots,1]^{\mathrm{T}}$ that is maximum, where $\mathbf{x}\in\{0,1\}$. Next, we prove $|\mathbf{x}_k^*|\le|\mathbf{x}_{k-1}^*|$ by induction. First of all, $\mathbf{x}_k^*\le\mathbf{x}_1^*$. Suppose for the sake of induction that $|\mathbf{x}_{k-1}^*|\le|\mathbf{x}_{k-2}^*|$ where $k\in\mathbb{Z}^+$. Then if $LB^k=LB^{k-1}$, we have $|\mathbf{x}_k^*|\le|\mathbf{x}_{k-1}^*|$ directly. Else if $LB^k\ge LB^{k-1}$, then we have $|\mathbf{x}_k^*|=|argmin(MP(x_k))|\ge|argmin(MP(x_{k-1}))|=|\mathbf{x}_{k-1}^*|$ since x_k and x_{k-1} are the optimal and feasible solutions to the MP, respectively. □

Lemma 2: If $\mathbf{u}_k^*$ is an exact solution in (36), then as the increase of itertaion, $|\mathbf{u}_k^*|\ge|\mathbf{u}_{k-1}^*|$, leading to a non-decrease series of upper boundary.

Proof: Let $\mathbf{u}_k^*$ denote the uncertain variables of Algorithm 1 at iteration k. When $k=1$, in Line 13 of Algorithm 1, deriving $\mathbf{u}_1^*=[0,0,\ldots,0]^{\mathrm{T}}$ that is minimum, where $\mathbf{u}\in\{0,1\}$. Next, we prove $|\mathbf{u}_k^*|\ge|\mathbf{u}_{k-1}^*|$ by induction. First of all, $\mathbf{u}_k^*\ge\mathbf{u}_1^*$. Suppose for the sake of induction that $|\mathbf{u}_{k-1}^*|\ge|\mathbf{u}_{k-2}^*|$ where $k\in\mathbb{Z}^+$. Then if $UB^k=UB^{k-1}$, we have $|\mathbf{u}_k^*|\ge|\mathbf{u}_{k-1}^*|$ directly. Else if $UB^k\le UB^{k-1}$, then we have $|\mathbf{u}_k^*|=|argmax(S(u_k))|\le|argmax(S(u_{k-1}))|=|\mathbf{u}_{k-1}^*|$ since u_k and u_{k-1} are the optimal and feasible solutions to the problem (33), respectively. □

Theorem 1: Algorithm 1 converges to the ε-optimal value in finite iterations.

Proof: Since MP, i.e., Line 7 in Algorithm 1, is a relaxation to the problem (1) for all the numbers of iterations $k\in N$, the optimal objective value of MP, which is recorded as LB^k, is less than

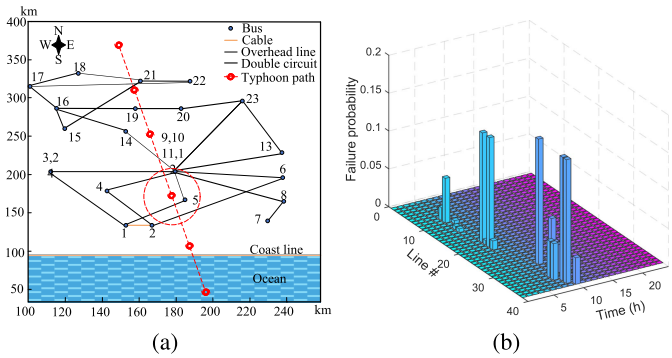

Fig. 4. (a) IEEE reliability test system under a hurricane. (b) Transmission line failure probability.

or equal to the optimal function value of the problem (1), i.e., $LB^k \leq \mathbf{c}^{\mathrm{T}}\mathbf{x}^* + Q(\mathbf{x}^*)$. Likewise since SP (36) is a relaxation of $\max_{\mathbf{u}\in\mathcal{U}(\mathbf{x})} \mathcal{Q}(\mathbf{x})$, $\mathbf{x}^k$ is a feasible solution. Further for the maximization problem $Q(\mathbf{x})$, $Q(\mathbf{x}^*) > Q(\mathbf{x}^k)$. Recall the updating rule of the UB which is $UB^k = \min\{\mathbf{c}^{\mathbf{T}}\mathbf{x}^k + \mathcal{Q}(\mathbf{x}^k), UB^{k-1}\}$, we have $\mathbf{c}^{\mathrm{T}}\mathbf{x}^* + Q(\mathbf{x}^*) \leq UB^k$.

We finally establish the ε-optimal value $\mathbf{x}^k$. According to $LB^k \leq \mathbf{c}^{\mathrm{T}}\mathbf{x}^* + Q(\mathbf{x}^*) \leq UB^k$ and the condition that Algorithm 1 terminates at $(UB^k - LB^k)/\max(UB^k, LB^k) \leq \varepsilon$, for the molecule we have $(UB^k - \mathbf{c}^{\mathrm{T}}\mathbf{x}^* - Q(\mathbf{x}^*)) \leq \varepsilon$. Recalling that the UB is also obtained by $UB^k = \mathbf{c}^{\mathbf{T}}\mathbf{x}^k + \mathcal{Q}(\mathbf{x}^k)$, we have $(\mathbf{c}^{\mathbf{T}}\mathbf{x}^k + \mathcal{Q}(\mathbf{x}^k) - \mathbf{c}^{\mathrm{T}}\mathbf{x}^* - Q(\mathbf{x}^*)) \leq \varepsilon$, which proves the ε-optimality of $\mathbf{x}^k$. Algorithm 1 converges in k iterations.

As a bounded polyhedron set, $\mathcal{U}$ admits finite extreme points. The generated $\mathbf{u}_k^*$ in iteration k belongs to a finite set with $|\mathcal{V}(\mathcal{U})|$ elements. As both $\mathbf{u}_k^*$ and $\mathbf{x}_k^*$ are bounded convergent series, according to Lemmas 1 and 2, Algorithm 1 converges in $\mathcal{O}(|\mathcal{V}(\mathcal{U})|)$ iterations when $|\mathbf{u}_k^* - \mathbf{u}_{k-1}^*| = 0$. □

IV. Case Study

In this section, case studies are conducted on the modified IEEE RTS-79 [33] and the two-area IEEE RTS-96 [40] under a hurricane to verify the merits of the proposed planning models and solution methods.

A. Case Description

A modified IEEE 24 bus reliability test system under one hurricane, as shown in Fig. 4(a). The test system is projected to a 150*200 km area approximately located within (30.52°N-32.32°N, 87.68°W-89.25°W). The hurricane is to be generated within the area (29.31°N-30.21°N, 86.64°W-90.29°W) at 02:00 am in the operating day. For this hurricane, the failure probability of each line across the hurricane periods is given in Fig. 4(b). The reference power is set to be 100MVA. The parameters for the generators, loads and transmission lines are referred to [41]. For the two-area IEEE RTS-96, which contains two equal areas, each of which being identical to the IEEE RTS-79 system, and three additional lines connecting the two areas. Assume that one of the areas is affected by a hurricane and the other is unaffected.

The parameters in the cases are set as $K = 2$, $VOLL = 4000$\$/MWh, $VOGC = 1000$\$/MWh, $\Delta t = 1$ h, $T = 24$, $\Pi = 0.001$. The cost of hardening each line c_{ij} is 6000\$ [42]. The optimization programs are coded in Matlab 2019b and solved by commercial solver CPLEX 12.10 and Gurobi 11.0.0. Numerical tests are conducted on a laptop with an Intel i9-12900H CPU and 16 GB of RAM. To demonstrate the effectiveness of the resilience enhancement strategy and modified C&CG algorithm proposed in this paper, several cases are constructed for comparative analysis as follows

- *Case I:* Two resilience enhancement measures, pre-disaster line hardening x_{ij} and post-disaster failure repair κ_{ij}^t, are both considered as benchmarks.
- *Case II:* Only pre-disaster line hardening measures are considered and post-disaster failure repair is not taken into account, i.e., (8) becomes $I_{ij}^t = I_{ij}^{t-1} - \gamma_{ij}^t$.
- *Case III:* The robust resilience enhancement (RRE) model based on RO is considered [25], where the unrealistic assumption exists that the hardened lines will definitely not be damaged during the hurricane[1].
- *Case IV:* The box uncertainty set is considered[2] [26], where there is no correlation between uncertain variables.
- *Case V:* Different algorithms are applied to the models for comparisons, including the Algorithm 1, the Benders + C&CG[3] [24], and C&CG-AOP algorithm[4] [27]. Notably, the benchmark algorithm is C&CG-AOP, which has no accelerating techniques for ordinary cases.
- *Case VI:* Cooperative games between line hardening and unit commitment plans.

B. Simulated Results and Discussions on IEEE RTS-79

1) Results Comparison Among Algorithms Under Case I: To evaluate the two resilience enhancement measures for the power system of hardening the transmission lines before the hurricane and repairing the failed lines after the hurricane, for the worst line failure scenario encompassing line damage before and after hardening, the repair results of Algorithm 1 (A1), the Benders + C&CG algorithm (A2), and the C&CG-AOP algorithm (A3) searched in the second stage of TRO under the same system parameters are shown in Fig. 5. Table I shows the reinforcement results of the three algorithms for the possible failed lines during the disaster. From Fig. 5(a), it can be observed the number of worst line faults searched by the improved C&CG algorithm proposed in this paper is 18. Note that, it can be seen from Table I that 10 of the 18 lines are hardened before the hurricane, and the eight lines are not hardened. We find that, after reinforcing these eight transmission lines, failures still occurred during the arrival

[1]The scenario labeled as case 4 in Fig. 3 does not exist.

[2]$\gamma_{ij}^{t,0} \leq x_{ij}$ and without uncertain variable γ_{ij}^t.

[3]The Benders + C&CG algorithm can solve the TRO with DDU [24]. Since the endogenous uncertainty is synonymous with DDU [13], Benders + C&CG is applicable to solve endogenous uncertainty case for the model formulated in this paper.

[4]The C&CG-AOP algorithm treats the uncertainty set $Cu \leq g$ as $Cu \leq g + Nx$ by adding endogenous cuts to the master problem of the outer and inner levels. So C&CG-AOP is applicable to solve endogenous uncertainty case for the model formulated in this paper.

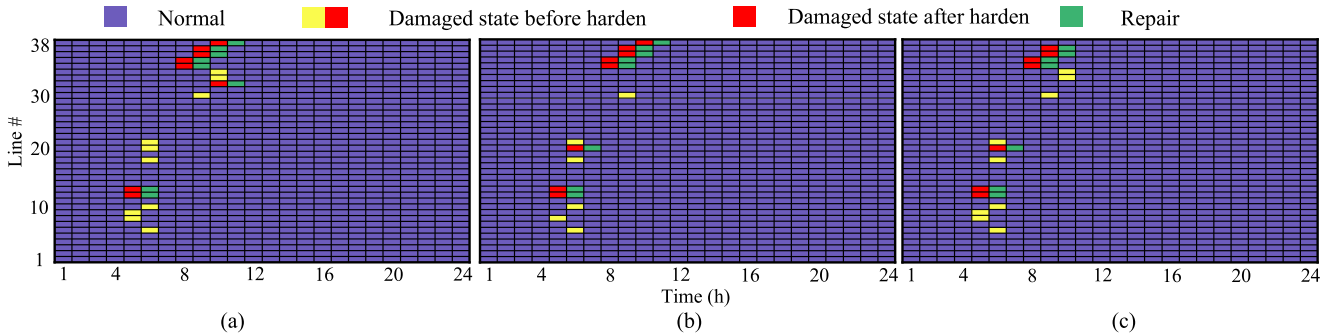

Fig. 5. States of normal operation, damaged before hardening, damaged after hardening, and repaired of transmission lines based on the worst case under Case IV. (a) Solved by the algorithm proposed in this paper. (b) Solved by the Benders + C&CG algorithm. (c) Solved by the C&CG-AOP algorithm.

TABLE I
RESULTS OF LINES HARDENED FOR MODEL WITH REPAIR

	A1	A2	A3
Hardened #	3-9,4-9,5-10,6-10 11-13,12-13,12-23 16-19,18-21,18-21	3-9,4-9 6-10,11-13 12-23,16-19	3-9,4-9,5-10,6-10 11-13,12-23,16-19 18-21,18-21
Unhardened #	Other lines	Other lines	Other lines

∗ Line 18-21 is the double circuit.

TABLE II
RESULTS OF LINES HARDENED FOR MODEL WITHOUT REPAIR

	A1	A2	A3
Hardened #	3-9,5-10,6-10,8-9 8-10,11-13,12-13,12-23 16-19,17-22,18-21 18-21,19-20,19-20 20-23,20-23,21-22	3-9,5-10,6-10 8-9,8-10,11-13 12-23,16-19 17-22,18-21 19-20,20-23	3-9,5-10,6-10 8-9,8-10,11-13 12-23,16-19,17-22 18-21,19-20,19-20 20-23,20-23
Unhardened #	Other lines	Other lines	Other lines

∗ Lines 18-21, 19-20, and 20-23 are the double circuit.

of hurricanes. That is, transmission lines can still be damaged by hurricanes after reinforcement, which has practical implications in engineering applications. The system is not hardened for these eight lines to meet the goal of cost optimization. Nevertheless, it is observed in Fig. 5(a) that the maintenance measures manage to repair the eight lines to ensure timely restoration of load power supply after the hurricane. The interplay of failed line hardening and repair measures still shows a positive effect in preventing power outages during extreme weather.

In addition, the number of the worst-case failed lines searched by the Benders + C&CG and the C&CG-AOP algorithm in the second stage are 11 and 16, which are 38.88% and 11.11% less than that by Algorithm 1, respectively. According to the worst-case scenario of transmission line failure during the hurricane, as shown in Fig. 5(b) and Fig. 5(c), the failed lines should be precisely hardened before the arrival of a hurricane. Likewise, as shown in Table I, the model solved by the Benders + C&CG and C&CG-AOP algorithm is less accurately in hardening the lines before a hurricane attack.

These results indicate that solving the TRO model with the endogenous uncertainty set proposed in this paper for enhancing power system resilience by Algorithm 1 can: (1) achieve more accurate situation awareness of the worst-case line failure scenario under a given criterion and provide more specific preventive guidance for operators, as shown in Fig. 5(a); and (2) provide the power system operator with accurate fault line prevention hardening and repair strategies to reduce economic losses.

2) Results Comparison Among Algorithms Under Case II: To evaluate only hardening measures for possible failed lines during hurricane, the failed lines in the worst-case scenario searched by Algorithm 1 (A1), the Benders + C&CG algorithm (A2), and the C&CG-AOP algorithm (A3) respectively in the second stage of TRO under the same system parameters are shown in Fig. 6. Table II shows the results of the three algorithms for the reinforcement of possible failed lines. The right half of Table III presents the results of different costs and worst-case scenarios for lines under hurricanes obtained by the three algorithms respectively for solving the model in Case II. The number of failed lines searched by Algorithm 1 in the second stage is 19, while the Benders + C&CG and C&CG-AOP algorithms have 14 and 16 failed lines, accounting for 73.68% and 84.21% of Algorithm 1, respectively.

Additionally, the cost results for each part of the power system solved by the Algorithm 1, Benders + C&CG, and C&CG-AOP algorithm in Case I and Case II are shown in Table III. The model solved in Table III takes the total cost of the algorithm proposed in this paper as a reference. In comparison with the repaired model, the errors of Benders + C&CG and C&CG-AOP are 0.08% and 0.03%, respectively, both less than 1%. Similarly, in comparison with the unrepaired model, the errors of Benders + C&CG and C&CG-AOP are 0.02% and 0.01%, also both less than 1%. Due to the *MIPGap* error in the solver used by the algorithms, it can be considered that the objective functions obtained by these three algorithms are roughly equal. The inability to detect lines with possible faults and take preventive measures will lead to more serious economic losses.

Finally, according to Fig. 6, it can be observed that even with hardening, the hardened lines may still experience faults and prolonged downtime in the absence of repair actions. This is the direct cause leading to a significant increase in the magnitude of load shedding and generator curtailment in the second stage. By examining the endogenous uncertainty relationship between unit reserve and post-reinforcement line faults, we

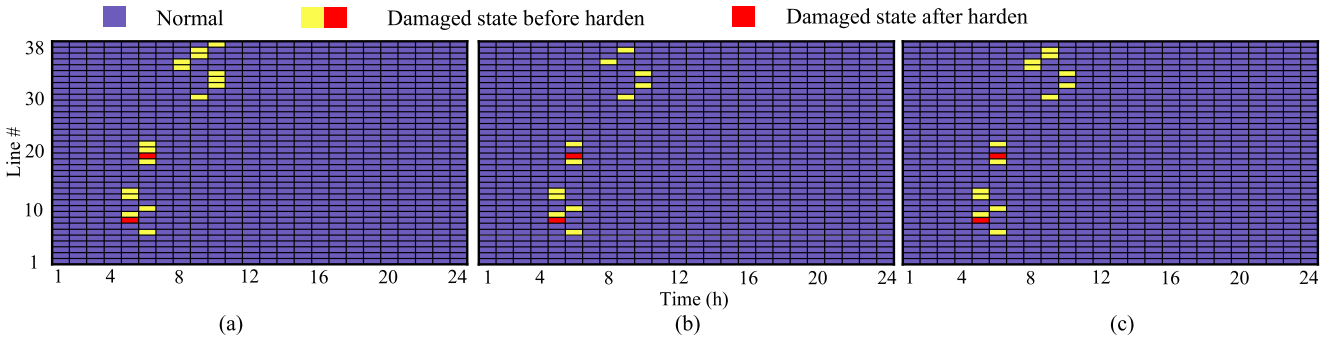

Fig. 6. States of normal operation and damaged before hardening of transmission lines based on the worst case under Case IV. (a) Solved by the algorithm proposed in this paper. (b) Solved by the Benders + C&CG algorithm. (c) Solved by the C&CG-AOP algorithm.

TABLE III
RESULTS OF DIFFERENT ALGORITHMS IN IEEE RTS-79

Results	Model with repair			Model without repair		
	Proposed	Benders + C&CG [24]	C&CG-AOP [27]	Proposed	Benders + C&CG [24]	C&CG-AOP [27]
Total cost($)	2799792.97	2777810.88	2809394.55	16698515.57	16670427.96	16708178.39
First stage cost($)	791192.97	769210.88	800794.55	898515.56	870427.96	908178.38
Start-up/shut-down cost($)	6215.51	6245.86	4070.28	6874.37	6537.12	1964.65
Fuel cost($)	711885.83	714423.30	729840.65	777470.75	778780.42	807520.65
Reserve cost($)	13091.63	12541.72	12883.62	13191.76	13110.42	14693.09
Hardening cost($)	60000	36000	54000	102000	72000	84000
Second stage cost($)	2008600.00	2008600.00	2008600.00	15800000.00	15800000.00	15800000.00
Load shedding cost($)	2008600.00	2008600.00	2008600.00	15800000.00	15800000.00	15800000.00
Generator curtailment cost($)	7.52×10^{-7}	5.74×10^{-8}	0.00	2.98×10^{-6}	3.41×10^{-8}	0.00
Number of failed lines	**18**	11	16	**19**	14	16

TABLE IV
RESULTS OF PERFORMANCE FOR DIFFERENT ALGORITHMS

Results	Solution algorithm		
	Proposed	Benders+C&CG [24]	C&CG-AOP [27]
Iteration	2	2	3
Gap (%)	0.00%	0.00%	0.00%
Computation time (s)	30.11	30.23	163.91
Number of failed lines	18	11	16

$*$ $Gap = (UB - LB) / \max(UB, LB)$.

derive the result that reserve operation is required for 05:00 and 06:00, i.e., $\varpi^5 = \varpi^6 = 1$.

3) Performance Comparison of Different Algorithms: In this part, the Algorithm 1, Benders + C&CG and C&CG-AOP algorithm are utilized for the optimization of Case I respectively, and the optimal results of different algorithms are displayed in Table IV. As described in Table III, the objectives of the three algorithms in both cases are approximately consistent, indicating the validity and correctness of the proposed algorithm. Since Algorithm 1 proposed in this paper is reverse thinking compared to the other two algorithms in searching for the worst scenario in the second stage, Algorithm 1 reaches a better perception of the risk, i.e., the number of failed lines, when searching for the optimal starting from the lowest system risk. Simultaneously, when the convergence gaps of the three algorithms all reach 0.00%, Algorithm 1 exhibits fewer iterations and shorter computation time, providing a significant advantage in preparing for disaster risk reduction plans.

These results show that Algorithm 1 proposed in this paper outperforms the Benders + C&CG and C&CG-AOP algorithm in terms of situation awareness of possible failed lines during hurricane arrival. The TRO model with endogenous uncertainty set solved by Algorithm 1 can provide more practical predictive guidance for the power system to operate strongly and reliably in the face of hurricanes. By observing the result of the first iteration of the hardening, i.e., x_{ij}^1, it is found that Algorithm 1 generated an efficient initial solution.

4) Sensitivity Analysis on K and Threshold Π: Using Algorithm 1 to solve the scenario under Case II. As shown in (7) and (10), the parameter K and the line failure threshold Π play an essential role in the preparation of dispatch. The worst line failure scenario with different thresholds Π is given in Fig. 7. As shown in Fig. 7(a), lines (11–13) and (12–13) failed at 06:00, and lines (16–19) and the double circuit (20–23) failed at 09:00, causing the line to stop running. Also, as shown in Fig. 7(b), (c), and (d), the location, time, and number of worst-case line failures upon hurricane arrival change for different thresholds Π. These results indicate that probability threshold Π can be used to detect the time, place, and number of failures that would occur for lines in the worst case.

Fig. 8 illustrates the costs associated with different maximum numbers of line failures K, where "H" means the line hardening cost ($\times10^5$), "T" means the power system's operating total cost ($\times10^7$), and "L" means the load shedding penalty cost ($\times10^0$). It is observed from Fig. 8 that the hardening cost is decreasing as K is increasing, while the total system operating cost is slowly increasing. However, the load shedding of the system is

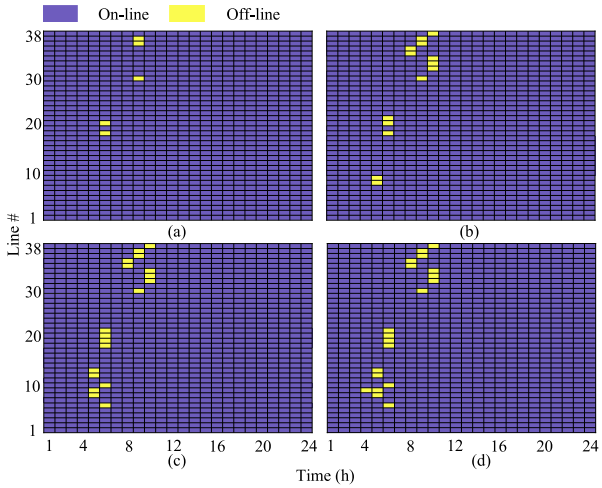

Fig. 7. Worst line failure scenario in Case II. (a) $\Pi = 10^{-1}$. (b) $\Pi = 10^{-2}$. (c) $\Pi = 10^{-3}$. (d) $\Pi = 10^{-4}$.

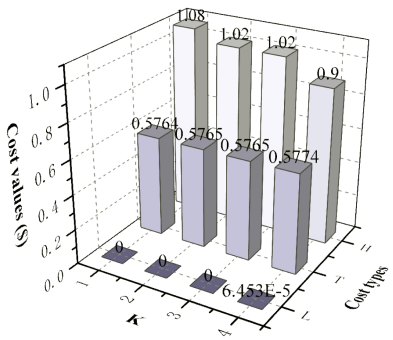

Fig. 8. The relevant costs with different K.

TABLE V
COMPARISON OF DIFFERENT MODELING FRAMEWORK

Strategy	Correlation among variables	Hardened lines damaged	Repair measure
Case I	✓	✓	✓
Case II	✓	✓	×
Case III	✓	×	✓
Case IV	×	×	×

always at a zero or near-zero value. Line hardening measures still demonstrate a positive effect in preventing power outages under hurricanes. These results can help system operators assess readiness under various K and arrange resources for preventive hardening.

5) Comparison Analysis of Various Correlation Uncertainty Sets: The three endogenous uncertainty sets are introduced into the proposed TRO model for comparison and analysis. The differences are shown in Table V, which focuses on the correlation among variables, hardened line failures and repair measures. Our proposed models are Cases I and II. Case III is derived from the RRE model based on RO in [25], where the hardened lines will definitely not be damaged. Case IV is taken from the boxed uncertainty set in [26], where none of the three aspects are in Table V.

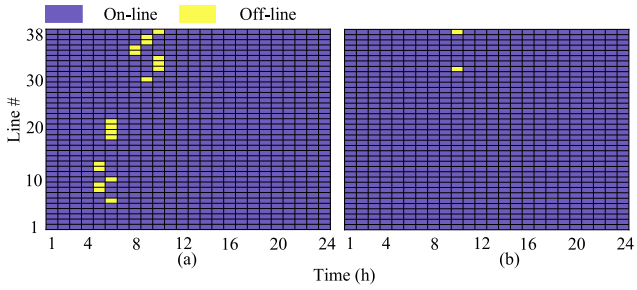

Fig. 9. Worst line failure scenario. (a) Case III. (b) Case IV.

TABLE VI
COOPERATIVE GAMES BETWEEN LINE HARDENING AND UC PLANS

Strategy		Cost		
Line Hardening	UC	First stage		Second stage
		Line Hardening	UC	
✓	✓	60000.00	2739792.97	**2008600.00**
×	✓	0.00	782990.36	45057155.00
✓	×	36000.00	0.00	215517000.00
×	×	0.00	0.00	226860000.00

The bold value indicative of their generation by the proposed approach.

The results of Case I and Case II solved by the modified C&CG algorithm are shown in Table III. The results of the worst case scenarios in Case III and Case IV for the failure situation of the lines are shown in Fig. 9, and their total costs are $\$8.2436 \times 10^5$ and $\$7.5047 \times 10^5$, respectively. For the faulty lines depicted in Fig. 9, the system underwent comprehensive reinforcement before the disaster, and the reinforced lines are not prone to further faults when the hurricane arrives. Therefore, describing the impact of hurricanes on transmission lines using Cases I and II is more realistic, effectively reducing uncertainty when formulating disaster prevention and mitigation plans based on actual scenarios.

C. Cooperative Games Between Line Hardening and UC Plans

To evaluate the contribution of the proposed resilience enhancement strategies, namely, line reinforcement and UC plans, this subsection performs cooperative game experiments on line reinforcement and UC schemes, as shown in Table VI.

Table VI illustrates four scenarios resulting from the combination of two strategies. It is observed that the cost of the combination strategy proposed in this paper is reduced by $\$4.30 \times 10^7$, $\$2.14 \times 10^8$ and $\$2.25 \times 10^8$ for the second stage compared to the other three combinations. Since the cost of the second stage involves load shedding and generator curtailment, the strategy proposed in this paper is effective and improves the system resilience.

D. Simulated Results and Discussions on IEEE RTS-96

To evaluate the scalability of the proposed resilience enhancement method, further case studies are conducted based on Case I solved by Algorithm 1 (A1), the Benders + C&CG (A2), and the C&CG-AOP (A3) in the two-area IEEE RTS-96 system. The

TABLE VII
RESULTS OF DIFFERENT ALGORITHMS IN TWO-AREA IEEE RTS-96

Results	Solution algorithm		
	A1	A2 [24]	A3 [27]
Total cost($)	43022487.79	43039189.06	43038521.79
First stage cost($)	1517572.79	1512624.81	1514906.82
Start-up/shut-down cost($)	12778.75	14492.89	13054.18
Fuel cost($)	1473740.41	1473617.68	1476675.18
Reserve cost($)	25053.63	24514.23	25177.46
Hardening cost($)	18000	0.00	0.00
Second stage cost($)	**41504915.00**	41526564.25	41523614.98
Load shedding cost($)	39829560.00	39829584.00	39829560.00
Generator curtailment cost($)	1675355.00	1696980.25	1694054.98
Number of failed lines	**18**	15	17

The bold values are indicative of their generation by the proposed approach.

simulation results obtained by different algorithms for Case I are given in Table VII. As shown in Table VII, the relative errors in the total costs for A1, A2, and A3 are all within the range of 1%, indicating that they can be regarded as approximately equal. However, the A1 proposed in this paper has the lowest cost for the second stage and senses up to 18 failed transmission lines. The number of the worst-case failed lines searched by A2 and A3 in the second stage are 15 and 17, which are 16.67% and 5.56% less than that by A1, respectively. Notably, all three algorithms involve the generator curtailment cost, as the repair time is set to 8 hours in this case. This is attributed to the failure in promptly repairing the persisting faults in the lines, consequently resulting in the occurrence of generator curtailment. Nevertheless, the results in Table VII show that solving the TRO model Case I with an endogenous uncertainty set by A1 can achieve more accurate situational awareness of the worst-case scenarios of line failures under the given criterion. This provides more specific preventive guidance for operators.

In terms of computational efficiency, the three algorithms take 233.17 s, 566.83 s, and 1003.45 s respectively to get convergent results the model in Table VII. Given the NP-hardness nature of the first stage, accurately predicting computational time is challenging. Nonetheless, our findings suggest that the proposed algorithms provide an efficient solution method. Note that if the second stage is modeled as MIP, the computation time of the algorithm will be significantly increased. In future research, a solution algorithm for NP-hard cases in the second stage shall be developed.

V. CONCLUSION

This paper proposed a resilient UC for transmission lines hardening toward hurricanes. The coupling between hardening decision, UC reserve decision, and line operation states was constructed as an endogenous uncertainty set. Meanwhile, the repair and failure operations were introduced to the endogenous uncertainty set, and a TRO problem was presented to balance economic efficiency and robustness. An improved C&CG algorithm was devised to solve the TRO problem. Simulations were performed on modified IEEE RTS-79 and two-area IEEE RTS-96 under a hurricane. The results demonstrated that the proposed second-stage recourse problem solved by the improved C&CG algorithm could well identify the failures on transmission lines under endogenous uncertainties. The failed lines were hardened or repaired to enhance the resilience. Apart from the refining of generator resources and transmission networks, we will investigate energy storage resources within the power system in the future, such as mobile energy storage systems, to resist hurricanes.

REFERENCES

[1] M. Mahzarnia, M. P. Moghaddam, P. T. Baboli, and P. Siano, "A review of the measures to enhance power systems resilience," *IEEE Syst. J.*, vol. 14, no. 3, pp. 4059–4070, Sep. 2020.

[2] S. Liu, T. Zhao, X. Liu, Y. Li, and P. Wang, "Proactive resilient day-ahead unit commitment with cloud computing data centers," *IEEE Trans. Ind. Appl.*, vol. 58, no. 2, pp. 1675–1684, Mar./Apr. 2022.

[3] H. Xiong, Y. Shi, Z. Chen, C. Guo, and Y. Ding, "Multi-stage robust dynamic unit commitment based on pre-extended -fast robust dual dynamic programming," *IEEE Trans. Power Syst.*, vol. 38, no. 3, pp. 2411–2422, May 2023.

[4] M. Panteli, D. N. Trakas, P. Mancarella, and N. D. Hatziargyriou, "Boosting the power grid resilience to extreme weather events using defensive islanding," *IEEE Trans. Smart Grid*, vol. 7, no. 6, pp. 2913–2922, Nov. 2016.

[5] T. Ding, M. Qu, Z. Wang, B. Chen, C. Chen, and M. Shahidehpour, "Power system resilience enhancement in typhoons using a three-stage day-ahead unit commitment," *IEEE Trans. Smart Grid*, vol. 12, no. 3, pp. 2153–2164, May 2021.

[6] B. Li, Y. Chen, W. Wei, S. Huang, and S. Mei, "Resilient restoration of distribution systems in coordination with electric bus scheduling," *IEEE Trans. Smart Grid*, vol. 12, no. 4, pp. 3314–3325, Jul. 2021.

[7] D. N. Trakas and N. D. Hatziargyriou, "Resilience constrained day-ahead unit commitment under extreme weather events," *IEEE Trans. Power Syst.*, vol. 35, no. 2, pp. 1242–1253, Mar. 2020.

[8] Y. Yang, J C.-H. Peng, C. Ye, Z.-S Ye, and Y. Ding, "A criterion and stochastic unit commitment towards frequency resilience of power systems," *IEEE Trans. Power Syst.*, vol. 37, no. 1, pp. 640–652, Jan. 2022.

[9] Z. Lu et al., "Risk-aware flexible resource utilization in an unbalanced three-phase distribution network using SDP-based distributionally robust optimal power flow," *IEEE Trans. Smart Grid*, vol. 15, no. 3, pp. 2553–2569, May 2024.

[10] S. Poudel and A. Dubey, "Critical load restoration using distributed energy resources for resilient power distribution system," *IEEE Trans. Power Syst.*, vol. 34, no. 1, pp. 52–63, Jan. 2019.

[11] H. Wu, Y. Xie, Y. Xu, Q. Wu, C. Yu, and J. Sun, "Robust coordination of repair and dispatch resources for post-disaster service restoration of the distribution system," *Int. J. Elect. Power Energy Syst.*, vol. 136, 2022, Art. no. 107611.

[12] T. H. Bhuiyan, H. R. Medal, and S. Harun, "A stochastic programming model with endogenous and exogenous uncertainty for reliable network design under random disruption," *Eur. J. Oper. Res.*, vol. 285, no. 2, pp. 670–694, 2020.

[13] W. Feng, Y. Feng, and Q. Zhang, "Multistage robust mixed-integer optimization under endogenous uncertainty," *Eur. J. Oper. Res.*, vol. 294, no. 2, pp. 460–475, 2021.

[14] Y. Su, Y. Zhang, F. Liu, S. Feng, Y. Hou, and W. Wang, "Robust dispatch with demand response under decision-dependent uncertainty," in *Proc. IEEE Sustain. Power Energy Conf.*, 2020, pp. 2122–2127.

[15] W. Zhang et al., "Transmission defense hardening against typhoon disasters under decision-dependent uncertainty," *IEEE Trans. Power Syst.*, vol. 38, no. 3, pp. 2653–2665, May 2023.

[16] T. Zhao, H. Zhang, X. Liu, S. Yao, and P. Wang, "Resilient unit commitment for day-ahead market considering probabilistic impacts of hurricanes," *IEEE Trans. Power Syst.*, vol. 36, no. 2, pp. 1082–1094, Mar. 2021.

[17] R. Chen and J. Luedtke, "On sample average approximation for two-stage stochastic programs without relatively complete recourse," *Math. Program.*, vol. 196, pp. 719–754, 2022.

[18] B. Zeng and L. Zhao, "Solving two-stage robust optimization problems using a column-and-constraint generation method," *Operations Res. Lett.*, vol. 41, no. 5, pp. 457–461, 2013.

[19] R. Rahmaniani, S. Ahmed, T. G. Crainic, M. Gendreau, and W. Rei, "The Benders dual decomposition method," *Operations Res.*, vol. 68, no. 3, pp. 878–895, 2020.

[20] W. Yin, S. Feng, and Y. Hou, "Stochastic wind farm expansion planning with decision-dependent uncertainty under spatial smoothing effect," *IEEE Trans. Power Syst.*, vol. 38, no. 3, pp. 2845–2857, May 2023.
[21] L. Qiu, Y. Dan, X. Li, and Y. Cao, "Decision-dependent distributionally robust integrated generation, transmission, and storage expansion planning: An enhanced benders decomposition approach," *IET Renewable Power Gener.*, vol. 17, no. 14, pp. 3442–3456, 2023.
[22] Y. Zhang, F. Liu, Y. Su, Y. Chen, Z. Wang, and J. P. S. Catalão, "Two-stage robust optimization under decision dependent uncertainty," *IEEE/CAA J. Automatica Sinica*, vol. 9, no. 7, pp. 1295–1306, Jul. 2022.
[23] Y. Zhang, F. Liu, Z. Wang, Y. Su, W. Wang, and S. Feng, "Robust scheduling of virtual power plant under exogenous and endogenous uncertainties," *IEEE Trans. Power Syst.*, vol. 37, no. 2, pp. 1311–1325, Mar. 2022.
[24] B. Zeng and W. Wang, "Two-stage robust optimization with decision dependent uncertainty," 2022, *arXiv:2203.16484*.
[25] Y. Li, S. Lei, W. Sun, C. Hu, and Y. Hou, "A distributionally robust resilience enhancement strategy for distribution networks considering decision-dependent contingencies," *IEEE Trans. Smart Grid*, vol. 15, no. 2, pp. 1450–1465, Mar. 2024.
[26] C. Gu, J. Wang, and L. Wu, "Distributed energy resource and energy storage investment for enhancing flexibility under a TSO-DSO coordination framework," *IEEE Trans. Automat. Sci. Eng.*, Early access, May 15, 2023, doi: 10.1109/TASE.2023.3272532.
[27] H. Qiu, H. Long, W. Gu, and G. Pan, "Recourse-cost constrained robust optimization for microgrid dispatch with correlated uncertainties," *IEEE Trans. Ind. Electron.*, vol. 68, no. 3, pp. 2266–2278, Mar. 2021.
[28] "How emergency managers in the electric industry prepare for and react to hurricanes," 2021. [Online]. Available: https://drj.com/journal_main/how-emergency-managers-in-the-electric-industry-prepare-for-and-react-to-hurricanes/
[29] "Hurricane preparedness guide," 2024. [Online]. Available: https://www.generac.com/be-prepared/storms/emergency-planning
[30] Y. Shen, G. Wang, and J. Zhu, "Resilience improvement model of distribution network based on two-stage robust optimization," *Electric Power Syst. Res.*, vol. 223, 2023, Art. no. 109559.
[31] K. Garifi, E. S. Johnson, B. Arguello, and B. J. Pierre, "Transmission grid resiliency investment optimization model with SOCP recovery planning," *IEEE Trans. Power Syst.*, vol. 37, no. 1, pp. 26–37, Jan. 2022.
[32] M. J. Brennan and S. J. Majumdar, "An examination of model track forecast errors for hurricane ike (2008) in the gulf of Mexico," *Weather Forecasting*, vol. 26, no. 6, pp. 848–867, 2011.
[33] H. Zhang, L. Cheng, S. Yao, T. Zhao, and P. Wang, "Spatial–temporal reliability and damage assessment of transmission networks under hurricanes," *IEEE Trans. Smart Grid*, vol. 11, no. 2, pp. 1044–1054, Mar. 2020.
[34] M. Ouyang and L. Duenas-Osorio, "Multi-dimensional hurricane resilience assessment of electric power systems," *Struct. Saf.*, vol. 48, pp. 15–24, 2014.
[35] H. Li, X. Xiao, J. Zhang, and H. Yan, "Two-stage robust unit commitment with wind farms and pumped hydro energy storage systems under typhoons," in *Proc. IEEE 17th Int. Conf. Control, Automat., Robot. Vis.*, 2022, pp. 518–523.
[36] N. Li, C. Uçkun, E. M. Constantinescu, J. R. Birge, K. W. Hedman, and A. Botterud, "Flexible operation of batteries in power system scheduling with renewable energy," *IEEE Trans. Sustain. Energy*, vol. 7, no. 2, pp. 685–696, Apr. 2016.
[37] M. Mehrtash, F. Capitanescu, P. K. Heiselberg, T. Gibon, and A. Bertrand, "An enhanced optimal PV and battery sizing model for zero energy buildings considering environmental impacts," *IEEE Trans. Ind. Appl.*, vol. 56, no. 6, pp. 6846–6856, Nov./Dec. 2020.
[38] X. Qi, T. Zhao, X. Liu, and P. Wang, "Three-stage stochastic unit commitment for microgrids towards frequency security via renewable energy deloading," *IEEE Trans. Smart Grid*, vol. 14, no. 6, pp. 4256–4267, Nov. 2023.
[39] X. A. Sun et al. *Robust Optimization in Electric Energy Systems*. Berlin, Germany: Springer, 2021.
[40] C. Grigg et al., "The IEEE reliability test system-1996. A report prepared by the reliability test system task force of the application of probability methods subcommittee," *IEEE Trans. Power Syst.*, vol. 14, no. 3, pp. 1010–1020, Aug. 1999.
[41] P. M. Subcommittee, "IEEE reliability test system," *IEEE Trans. Power App. Syst.*, vol. PAS-98, no. 6, pp. 2047–2054, Nov. 1979.
[42] S. Ma, L. Su, Z. Wang, F. Qiu, and G. Guo, "Resilience enhancement of distribution grids against extreme weather events," *IEEE Trans. Power Syst.*, vol. 33, no. 5, pp. 4842–4853, Sep. 2018.

Xiang Yang received the B.S. degree in electrical engineering in 2022 from the School of Electrical Engineering, Xi'an University of Technology, Xi'an, China where he is currently working toward the Ph.D. degree in electrical engineering. His research interests include resilient power systems, transportation electrification, uncertainty quantification, and operation research.

Xinghua Liu (Senior Member, IEEE) received the B.S.degree from Jilin University, Changchun, China, in 2009 and the Ph.D. degree in automation from the University of Science and Technology of China, Hefei, China, in 2014. From 2014 to 2015, he was invited as a Visiting Fellow with RMIT University,Melbourne, VIC, Australia. From 2015 to 2018, he was a Research Fellow with the School of Electrical and Electronic Engineering, Nanyang Technological University, Singapore. Dr. Liu has has been with the Xi'an University of Technology, Xi'an, China, as a Professor, since 2018. His research interests include state estimation and control, intelligent systems, autonomous vehicles, cyber-physical systems, and robotic systems.

Tianyang Zhao (Senior Member, IEEE) received the B.Sc., M.Sc., and Ph.D. degrees in electrical engineering from North China Electric Power University, Beijing, China, in 2011, 2013, and 2017, respectively. From 2017 to 2020, he was a Postdoctoral Research Fellow with the Energy Research Institute, Nanyang Technological University, Singapore. From 2020 to 2022, he was an Associate Professor with Energy and Electricity Research Center, Jinan University, Guangzhou, China. He was a Researcher with the University of Bath, Bath, U.K., in 2022, and the Royal Institute of Technology, Stockholm, Sweden, in 2023. He is currently an Associate Professor with the School of Electrical Engineering, Xi'an Jiaotong University, Xi'an, China. His research interests include operations research and resilience.

Gaoxi Xiao (Senior Member, IEEE) received the B.S. and M.S. degrees in applied mathematics from Xidian University, Xi'an, China, in 1991 and 1994, respectively, and the Ph.D. degree in computing from Hong Kong Polytechnic University, Hong Kong, in 1998. He was an Assistant Lecturer with Xidian University during 1994–1995. He was a Postdoctoral Research Fellow with Polytechnic University, Brooklyn, NY, USA, in 1999, and a Visiting Scientist with the University of Texas at Dallas, Richardson, TX, USA, during 1999–2001. In 2001, he joined the School of Electrical and Electronic Engineering, Nanyang Technological University, Singapore, where he is currently an Associate Professor. His research interests include complex systems and complex networks, communication networks, smart grids, and system resilience and risk regulation.

Bangji Fan received the B.S. degree in electrical engineering and automation from Xi'an Polytechnic University, Xi'an, China, in 2018, and the M.S. degree in electrical engineering in 2021 from the Xi'an University of Technology, Xi'an, where he is currently working toward the Ph.D. degree in electrical engineering. His research interests include distribution system restoration, deep reinforcement learning, and resilient power grid.

Shengwei Liu (Graduate Student Member, IEEE) received the B.Eng. and M.Eng. degrees in electrical engineering from Guangdong University of Technology, Guangzhou, China, in 2017 and 2020, respectively. He is currently working toward the Ph.D. degree in electrical engineering with the Energy and Electricity Research Center, Jinan University, Zhuhai, China. His research interests include smart grid resilience and operation research.

Peng Wang (Fellow, IEEE) received the the B.Sc. degree in electronic engineering from Xian Jiaotong University, Xian, China, in 1978, the first M.Sc. degree in electrical engineering from the Taiyuan University of Technology, Taiyuan, China, in 1987, and the second M.Sc. and Ph.D. degrees in electrical engineering from the University of Saskatchewan, Saskatoon, SK, Canada, in 1995 and 1998, respectively. He is currently a Full Professor with the School of Electrical and Electronic Engineering with Nanyang Technological University, Singapore. His research interests include power system planning and operation, renewable energy planning, solar/electricity conversion system, and power system reliability analysis. He was an Associate Editor for IEEE TRANSACTIONS ON SMART GRID and the Guest Editor of *Journal of Modern Power Systems and Clean Energy* Special Issues on smart grids. He was also an Associate Editor for IEEE TRANSACTIONS ON POWER DELIVERY and the Guest Editor-in-Chief of *CSEE Journal of Power and Energy Systems* Special Issues on hybrid AC/DC grids for future power systems.